

DOI: 10.1002/cmdc.201300093

# E-64c-Hydrazide: A Lead Structure for the Development of Irreversible Cathepsin C Inhibitors

Hanna Radzey,<sup>[a, b]</sup> Markus Rethmeier,<sup>[a, c]</sup> Dennis Klimpel,<sup>[a]</sup> Maresa Grundhuber,<sup>[d]</sup> Christian P. Sommerhoff,<sup>[d]</sup> and Norbert Schaschke<sup>\*[a]</sup>

Cathepsin C is a papain-like cysteine protease with dipeptidyl aminopeptidase activity that is thought to activate various granule-associated serine proteases. Its exopeptidase activity is structurally explained by the so-called exclusion domain, which blocks the active-site cleft beyond the S2 site and, with its Asp1 residue, provides an anchoring point for the N terminus of peptide and protein substrates. Here, the hydrazide of (2S,3S)-*trans*-epoxysuccinyl-L-leucylamido-3-methylbutane (E-64c) ( $k_2/K_i = 140 \pm 5 \text{ M}^{-1} \text{ s}^{-1}$ ) is demonstrated to be a lead structure for the development of irreversible cathepsin C inhibitors.

The distal amino group of the hydrazide moiety addresses the acidic Asp1 residue at the entrance of the S2 pocket by hydrogen bonding while also occupying the flat hydrophobic S1'-S2' area with its leucine-isoamylamide moiety. Furthermore, structure-activity relationship studies revealed that functionalization of this distal amino group with alkyl residues can be used to occupy the conserved hydrophobic S2 pocket. In particular, the *n*-butyl derivative was identified as the most potent inhibitor of the series ( $k_2/K_i = 56\,000 \pm 1700 \text{ M}^{-1} \text{ s}^{-1}$ ).

## Introduction

Cathepsin C, also known as dipeptidyl peptidase I (DPPI), is a cysteine protease that belongs to family C1A of clan CA (papain superfamily) according to the classification scheme of the MEROPS database.<sup>[1,2]</sup> Using both peptide hormones<sup>[3,4]</sup> and synthetic peptides as substrates,<sup>[5,6]</sup> it has been well documented that this protease acts virtually exclusively as a dipeptidyl aminopeptidase with broad substrate specificity. Only few restrictions have been identified, that is, substrates with lysine and arginine in the P2 position, isoleucine and proline in the P1 position, and proline in the P1' position are not processed by cathepsin C.

From a structural point of view, cathepsin C is unique among the currently known eleven human cysteine cathepsins. The X-ray crystal structure revealed that this protease consists of four identical catalytically active subunits that assemble to a tetramer and are located, with their active-site clefts fully solvent exposed, at the corners of a tetrahedron.<sup>[7]</sup> Each subunit

is composed of three chains; the light and heavy chains together form the catalytic domain with a papain-like fold and harbor the residues of the catalytic diad (i.e. Cys234(25) and His381(159); papain numbering given in brackets). The third chain, derived from a portion of the propeptide, constitutes the so-called exclusion domain that blocks the active-site cleft binding sites beyond the S2 pocket and thus is responsible for the exopeptidase activity of the protease. Furthermore, the side chain carboxylic acid of the Asp1 residue of the exclusion domain, which is located near the entrance of the S2 pocket, acts as an anchoring point for the N-terminal  $\alpha$ -amino function of a peptide or protein substrate. The role of Asp1 governing substrate recognition and processing has been confirmed by the X-ray crystal structure of cathepsin C in complex with the dipeptide substrate-based inhibitor H-Gly-Phe-CHN<sub>2</sub>.<sup>[8]</sup> Recently, a detailed picture of the catalytic mechanism of substrate cleavage by cathepsin C was elucidated by Schneck et al. by applying a combination of pre-steady-state and steady-state kinetics and solvent kinetic isotope effects using the dipeptide substrate L-seryl-L-tyrosine 7-amido-4-methylcoumarin (H-Ser-Tyr-AMC).<sup>[9]</sup>

Cathepsin C is abundantly expressed in almost all mammalian tissues,<sup>[10,11]</sup> reflecting its nonspecific function in general lysosomal protein turnover. In addition, knock-out studies have implicated the protease in the activation of a variety of granule-associated serine proteases, among them the neutrophil-derived proteases cathepsin G, elastase, and proteinase 3,<sup>[12]</sup> the cytotoxic T lymphocyte-derived proteases granzyme A and B,<sup>[13]</sup> as well as the mast-cell-derived proteases chymase and tryptase.<sup>[14]</sup> Evidence that cathepsin C plays a role in the activation of tryptase was also obtained using the human mast cell line HMC-1 in combination with the selective irreversible

[a] H. Radzey, M. Rethmeier, D. Klimpel, Priv.-Doz. Dr. N. Schaschke  
Fakultät für Chemie, Universität Bielefeld  
Universitätsstr. 25, 33615 Bielefeld (Germany)  
E-mail: norbert.schaschke@uni-bielefeld.de

[b] H. Radzey  
Institut für Organische und Biomolekulare Chemie  
Georg-August-Universität Göttingen  
Tammannstr. 2, 37077 Göttingen (Germany)

[c] M. Rethmeier  
Fakultät für Chemie und Biochemie  
Ruhr-Universität Bochum  
Universitätsstr. 150, 44801 Bochum (Germany)

[d] M. Grundhuber, Prof. Dr. C. P. Sommerhoff  
Institut für Laboratoriumsmedizin  
Klinikum der Ludwig-Maximilians-Universität  
Nußbaumstr. 20, 80336 München (Germany)

inhibitor H-Gly-Phe-CHN<sub>2</sub>.<sup>[15]</sup> Based on the well-established role of granule-associated serine proteases in a variety of pro-inflammatory and immunologic processes, cathepsin C as their activator represents a potential therapeutic target for the treatment of related diseases, such as chronic obstructive pulmonary disease (COPD), cystic fibrosis, rheumatoid arthritis, and allergic asthma. This hypothesis is supported by the finding that cathepsin C knock-out mice seem to be protected against the detrimental actions of granule-associated serine proteases in several disease-related mouse models.<sup>[12,16–18]</sup> On the other hand, however, deficiency in cathepsin C due to a point mutation in the gene causes Papillion–Lefèvre syndrome (PLS), a rare genetic disease<sup>[19,20]</sup> characterized by periodontitis and hyperkeratosis on hands and feet.

Most of the cathepsin C inhibitors investigated so far are mimics of dipeptide substrates functionalized with an electrophilic moiety addressing the catalytic residue Cys 234 either in a reversible or irreversible fashion.<sup>[21,22]</sup> Bondebjerg et al. have extended this strategy for inhibitor design.<sup>[23]</sup> Thus, based on a semicarbazide scaffold, the authors developed inhibitors that allow for addressing the S1' and S2' binding pockets in addition to the S sites in a substrate-like fashion. Although (2*S*,3*S*)-oxirane-2,3-dicarboxylic acid has been extensively used as a thiol-reactive group for the development of irreversible cysteine cathepsin inhibitors,<sup>[24,25]</sup> until now, little is known about cathepsin C inhibitors based on this privileged electrophile. Here, we report the structure-based design, synthesis and evaluation of a series of (2*S*,3*S*)-oxirane-2,3-dicarboxylic acid hydrazide-based cathepsin C inhibitors. Moreover, the structure–activity relationships of this novel class of inhibitors were established.

## Results and Discussion

### E-64c-hydrazide as a lead structure for the development of irreversible cathepsin C inhibitors

The binding mode of (2*S*,3*S*)-*trans*-epoxysuccinyl-L-leucylamido-3-methylbutane (E-64c) along the active-site cleft of cathepsin B was elucidated in detail by X-ray crystallography (Figure 1).<sup>[26]</sup> The complex shows that the leucine residue of E-64c addresses the affinity-generating hydrophobic S2 binding pocket, which is highly conserved among the cysteine cathepsins, whereas the *iso*-amyl moiety interacts with the S3 binding pocket. In addition, the thiol-reactive epoxide moiety modifies the catalytic cysteine in a covalent manner. Because of the high degree of structural similarity, this binding mode is thought to be conserved for most of the known cysteine cathepsins. In the case of the structurally unique cathepsin C, however, the S3 pocket is blocked by the exclusion domain and thus E-64c is predicted to address the S' sites (Figure 2). Accordingly, the leucine residue and the *iso*-amyl moiety should interact with the S1' and S2' pockets, respectively, while leaving the affinity-generating S2 pocket unoccupied. This binding mode should result in a rather low second-order rate constant for the inhibition of cathepsin C by E-64c. Indeed, our kinetic measurements revealed that E-64c is a very weak irreversible

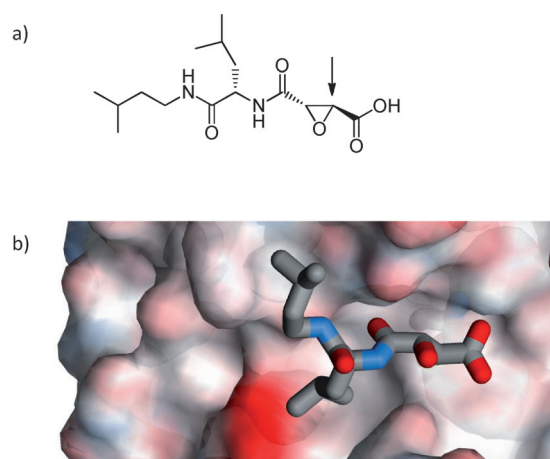


**Figure 1.** a) Chemical structure of E-64c. The arrow indicates the position where the active-site cysteine attacks the oxirane ring yielding the corresponding thioether upon ring opening. b) Covalent binding mode of E-64c along the active-site cleft of cathepsin B as determined by X-ray crystallography (PDB code: 1ITO).<sup>[26]</sup> Cathepsin B is shown in a transparent Connolly surface representation colored according to the electrostatic potential. E-64c and the catalytic cysteine are shown in stick representation (color code: C: gray, N: blue, and O: red; S: yellow; H atoms are omitted for clarity). Panel b) was prepared using Accelrys DS Visualizer v1.7.

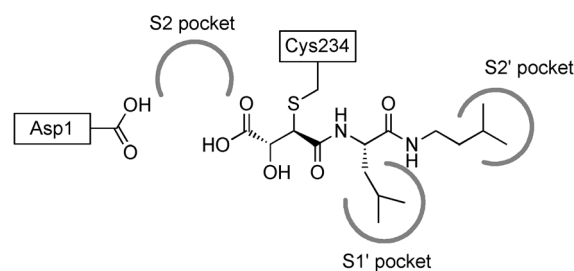
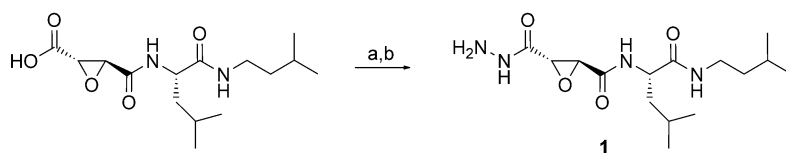


**Figure 2.** Schematic representation of the proposed covalent binding mode of E-64c along the active-site cleft of cathepsin C.

cathepsin C inhibitor with a  $k_2/K_i$  value of only  $23 \text{ M}^{-1} \text{ s}^{-1}$  (Table 1). For the structurally related 1-[*N*-[(L-3-*trans*-carboxyoxirane-2-carbonyl)-L-leucyl]amino]-4-guanidinobutane (E-64), a comparably low second-order rate constant for the inhibition of cathepsin C has been reported by Barrett et al. ( $k_2/K_i = 100 \text{ M}^{-1} \text{ s}^{-1}$ ).<sup>[27]</sup> According to the proposed binding mode of E-64c along the active-site cleft of cathepsin C, the carboxylic acid group of the (2*S*,3*S*)-oxirane-2,3-dicarboxylic acid portion should be positioned in near proximity to Asp1 of the exclusion domain. Thus, this functional group should be suitable for grafting a mimic of the substrate's N terminus that addresses Asp1 through hydrogen bonding. Using a structure-based approach, hydrazine was identified as an appropriate chemical entity that fulfills the structural requirements to act as such a mimic. To verify this concept, E-64c-hydrazide (**1**) was synthesized as outlined in Scheme 1. Briefly, E-64c, synthesized essentially following a procedure as described previously,<sup>[28]</sup> was coupled with *tert*-butyloxycarbonyl (Boc)-protected hydrazine. Upon cleavage of the protecting group using 95% aqueous trifluoroacetic acid (TFA), E-64c-hydrazide (**1**) was obtained. The



**Scheme 1.** Synthesis of E-64c-hydrazide (**1**). Reagents and conditions: a) Boc-NH-NH<sub>2</sub>·HCl, EDC, HOBt, DIEA, CHCl<sub>3</sub>, 3 h, RT; b) TFA/H<sub>2</sub>O (95:5, v/v), 0.5 h, RT, 22% over two steps.

second-order rate constant for the inhibition of cathepsin C by **1** is reported in Table 1. A comparison of the  $k_2/K_i$  value of E-64c ( $23 \text{ M}^{-1} \text{ s}^{-1}$ ) with that of corresponding hydrazide **1** ( $140 \text{ M}^{-1} \text{ s}^{-1}$ ) reveals a sixfold improvement in inhibitory potency induced by this modification. These findings are consistent with the design concept and classify E-64c-hydrazide (**1**) as a promising first-generation lead structure for the development of irreversible cathepsin C inhibitors.

### Structure-based considerations to improve the cathepsin C inhibitory potency

According to the proposed binding mode, the distal nitrogen of the hydrazide moiety addresses key residue Asp 1 at the entrance of the S2 site but still leaves the important affinity-generating pocket unoccupied. Similarly, as elucidated by the X-ray crystal structure of cathepsin C in complex with the dipeptide substrate-based inhibitor H-Gly-Phe-CHN<sub>2</sub>, the P2 glycine does not properly address the S2 binding pocket.<sup>[8]</sup> Rather, inspection of the structure reveals that the hydrophobic pocket is occupied by a series of structurally well-defined water molecules.<sup>[8]</sup> Therefore, for both enthalpic and entropic reasons, it was important to occupy this S2 pocket with an appropriate hydrophobic moiety to improve the inhibitory potency of our lead structure. This prompted us to build a model of E-64c-hydrazide (**1**) bound along the active-site cleft of cathepsin C (Figure 3). Inspection of this model predicts that the distal nitrogen of the hydrazide moiety is suited for functionalization with unbranched and branched alkyl residues in order to occupy the S2 binding pocket.

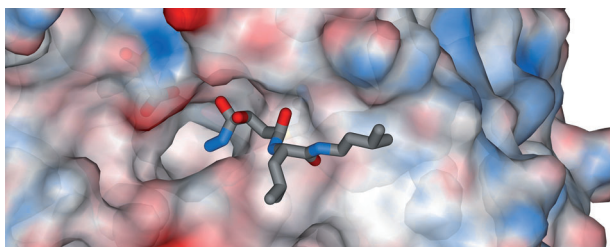
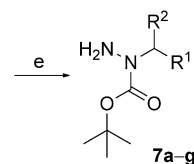
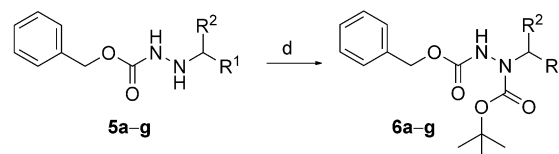
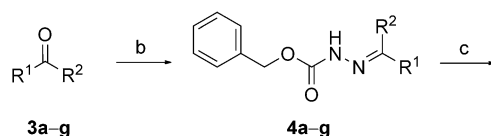
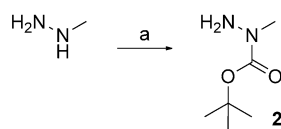


**Figure 3.** Model of the covalent binding mode of E-64c-hydrazide (**1**) along the active-site cleft of a subunit of the cathepsin C tetramer. The cathepsin C subunit is shown in a transparent Connolly surface representation colored according to the electrostatic potential. E-64c-hydrazide (**1**), Asp 1, and Cys 234 are shown in stick representation (color code: C: gray, N: blue, and O: red; S: yellow; H atoms are omitted for clarity). Figure 3 was prepared using Accelrys DS Visualizer v1.7.

### Synthesis of E-64c-hydrazide-based cathepsin C inhibitors

To identify an optimal hydrazine-based ligand for the S2 binding pocket, a set of alkylhydrazine building blocks with systematically varying steric demand was synthesized. To allow for selective

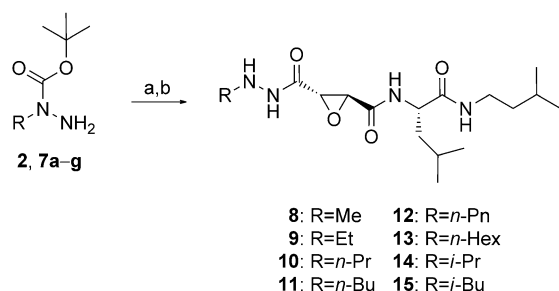
coupling of these S2 ligands with E-64c, Boc protection at the alkylated hydrazine nitrogen was employed. In particular, methylhydrazine could be directly Boc-protected following a procedure described by Busnel et al. yielding 1-methylhydrazinecarboxylic acid *tert*-butyl ester (**2**, Scheme 2).<sup>[29]</sup> However,



- 3a–7a:** R<sup>1</sup> = Me, R<sup>2</sup> = H  
**3b–7b:** R<sup>1</sup> = Et, R<sup>2</sup> = H  
**3c–7c:** R<sup>1</sup> = *n*-Pr, R<sup>2</sup> = H  
**3d–7d:** R<sup>1</sup> = *n*-Bu, R<sup>2</sup> = H  
**3e–7e:** R<sup>1</sup> = *n*-Pn, R<sup>2</sup> = H  
**3f–7f:** R<sup>1</sup> = Me, R<sup>2</sup> = Me  
**3g–7g:** R<sup>1</sup> = *i*-Pr, R<sup>2</sup> = H

**Scheme 2.** Synthesis of alkylhydrazine-based S2 ligand building block **2** and **7a–g**. Reagents and conditions: a) Boc<sub>2</sub>O, CHCl<sub>3</sub>, 0.5 h at 0 °C, then 24 h at RT, 84%; b) ZHN-NH<sub>2</sub>, toluene, 2 h at 60 °C, then 24 h at RT, 72–99%; c) DIBAL, THF, 2 h at –78 °C, then 2 h at –40 °C → –10 °C (aldimines) or NaBH<sub>4</sub>, THF, 2 h at RT (ketimine); d) Boc<sub>2</sub>O, NaOH, dioxane/H<sub>2</sub>O (1.6:1, v/v), 16 h, RT, 17–87% over two steps; e) H<sub>2</sub>, 10% Pd/C, EtOH, 16 h, RT, 21–94%.

our attempts to extend this strategy on other alkylhydrazines were not successful. Therefore, an alternative approach was chosen. Essentially according to a route described by Bailey et al.,<sup>[30]</sup> benzyloxy-carbonyl (Z)-protected hydrazine was first reacted with selected aldehydes **3a–e,g** and ketone **3f** (Scheme 2). Next, a reductive amination was performed on the imine intermediates using diisobutylaluminum hydride (DIBAL) for aldimines **4a–e,g** and sodium borohydride for ketimine **4f**. Subsequent Boc protection and cleavage of the Z protecting group yielded a set of structurally diverse 1-alkylhydrazinecar-



**Scheme 3.** Synthesis of E-64c-hydrazide-based cathepsin C inhibitors. *Reagents and conditions:* a) E-64c, TBTU, DIEA, CH<sub>2</sub>Cl<sub>2</sub>, 3 h, RT; b) TFA/H<sub>2</sub>O (95:5, v/v), 0.5 h, RT, 19–83% over two steps.

boxylic acid *tert*-butyl esters (**7a–g**). Finally, E-64c was coupled with the S2 ligand building blocks, yielding upon cleavage of the Boc group E-64c-hydrazide-based cathepsin C inhibitors **8–15** (Scheme 3).

### Inhibitory profiles of E-64c-alkylhydrazide-based cathepsin C inhibitors

The second-order rate constants for the inhibition of cathepsin C by E-64c-alkylhydrazides **8–15** are summarized in Table 1. First, a comparison of the  $k_2/K_i$  values of these inhibitors with lead compound **1** reveals that almost all of them exhibit improved inhibitory potency. This finding is in full agree-

Compd	$k_2/K_i$ [M <sup>-1</sup> s <sup>-1</sup> ] <sup>[a]</sup>	Compd	$k_2/K_i$ [M <sup>-1</sup> s <sup>-1</sup> ] <sup>[a]</sup>
E-64c	23 ± 1	<b>11</b>	56 000 ± 1700
<b>1</b>	140 ± 5	<b>12</b>	29 000 ± 1000
<b>8</b>	50 ± 1	<b>13</b>	1300 ± 70
<b>9</b>	2100 ± 50	<b>14</b>	9600 ± 200
<b>10</b>	23 000 ± 600	<b>15</b>	21 000 ± 400

[a] Data represent the mean ± standard error (SE),  $n \geq 10$ .

ment with the applied structure-based approach to augment the potency of lead compound **1** by addressing the hydrophobic S2 pocket in a proper manner (see above). Furthermore, the obtained data show a clear structure–activity relationship for the investigated S2–P2 interaction. In particular, starting from inhibitor **8** (Me residue,  $k_2/K_i = 52 \text{ M}^{-1} \text{ s}^{-1}$ ), the inhibitory potency increase significantly with increasing length of the *n*-alkyl chain reaching its maximum with inhibitor **11** (*n*-Bu residue,  $k_2/K_i = 56 000 \text{ M}^{-1} \text{ s}^{-1}$ ). Further elongation of the *n*-alkyl chain (**12** and **13**), however, is accompanied with a loss in inhibitory potency. Moreover, comparison of the inhibitor pairs **10** (*n*-Pr) and **14** (*i*-Pr) as well as **11** (*n*-Bu) and **15** (*i*-Bu), respectively, reveals that unbranched alkyl residues are superior to the structurally related branched analogues as S2 ligands.

In order to assess the effects of these modifications to E-64c on the inhibitory profile within the group of human cysteine

cathepsins, cathepsin L was selected for initial selectivity studies. The second-order rate constants for the inhibition of cathepsin L by E-64c, lead compound **1**, and optimized inhibitor **11** were determined (Table 2). Comparison of the  $k_2/K_i$  value of E-64c with that of inhibitor **11** clearly reveals that the 2400-fold increase in affinity for cathepsin C is simultaneously accompanied by a 24-fold loss in affinity for cathepsin L. Thus, implementation of the *n*-butylhydrazine-based S2 ligand in E-64c has shifted the inhibitory profile from a virtually selective cathepsin L inhibitor into a remarkable potent cathepsin C inhibitor with threefold selectivity for cathepsin C.

Compd	$k_2/K_i$ [M <sup>-1</sup> s <sup>-1</sup> ] <sup>[a]</sup>	
	Cathepsin C	Cathepsin L
<b>11</b>	56 000 ± 1700	17 000 ± 600
<b>1</b>	140 ± 5	33 000 ± 800
E-64c	23 ± 1	410 000 ± 16 000

[a] Data represent the mean ± standard error (SE),  $n \geq 10$ .

### Conclusions

Using a structure-based approach, we have identified E-64c-hydrazide (**1**) as a lead compound for the development of irreversible cathepsin C inhibitors. Furthermore, a focused structure–activity relationship study revealed that functionalization of the distal nitrogen of the hydrazide moiety with a *n*-butyl residue allows the addressing of the affinity-generating hydrophobic S2 pocket in an optimal manner. The resulting inhibitor (**11**), which in comparison to lead compound **1** has a superior affinity/selectivity profile, is currently in use as a starting point for the identification of optimized S1'–S2' ligands.

### Experimental Section

Solvents and reagents were of the highest purity commercially available and were used without further purification. 1-Ethyl-3-(3-dimethylaminopropyl)carbodiimide (EDC), *N,N,N',N'*-tetramethyl-*O*-(benzotriazol-1-yl)uronium tetrafluoroborate (TBTU), and hydroxybenzotriazole (HOBT) were purchased from Iris Biotech (Marktredwitz, Germany), and methylhydrazine, hydrazinecarboxylic acid *tert*-butyl ester, hydrazinecarboxylic acid benzyl ester, and di-*tert*-butyl dicarbonate (Boc<sub>2</sub>O) from Sigma–Aldrich. E-64c was synthesized following a procedure described previously,<sup>[28]</sup> and 1-methylhydrazine-carboxylic acid *tert*-butyl ester (**2**) was prepared as described by Busnel et al.<sup>[29]</sup> Precipitated compounds were collected by centrifugation using a Labofuge I from Heraeus Christ GmbH (Hanau, Germany).

<sup>1</sup>H NMR spectra were recorded on a DRX 500 (500 MHz) or an Avance 600 (600 MHz) spectrometer from Bruker. Electrospray ionization (ESI) mass spectrometry (MS) was performed on a Bruker Esquire 3000 quadrupole ion trap mass spectrometer, high-resolution mass spectrometry (HRMS) was performed on a APEX III FT-ICR (MALDI) or a micrOTOF (ESI) mass spectrometer from Bruker Daltonics. Thin layer chromatography (TLC) was performed on silica

gel 60 plates with fluorescence indicator F<sub>254</sub>, and flash chromatography was carried out using silica gel 60 (230–400 mesh) both from VWR International GmbH (Darmstadt, Germany). The compounds on the TLC plates were visualized with UV light ( $\lambda = 254$  nm) using a MinUVIS lamp from Desaga (Heidelberg, Germany) with ninhydrin (hydrazines) or with 4-(4-nitrobenzyl)pyridine (oxiranes).<sup>[31]</sup>

Analytical reverse phase (RP)-HPLC was performed with a system from Thermo Separation Products using a column from Macherey-Nagel (type ET 125/4 Nucleosil 100-5 C18 PPN, column size 125 × 4 mm) and eluting at a flow rate of 1.5 mL min<sup>-1</sup> with the gradient: 0–1 min, isocratic A/B (100:0); 1–14 min, linear gradient from A/B (100:0) to A/B (0:100) (eluent A: H<sub>2</sub>O/MeCN/TFA, 95:5:0.1 v/v/v, eluent B: MeCN/H<sub>2</sub>O/TFA, 95:5:0.1 v/v/v). Preparative RP-HPLC was performed with a LaChrome Type HPLC system from Merck Hitachi using a column from Phenomenex (Type Jupiter 10  $\mu$ m, C18, 300 Å, 250 × 21.20 mm), eluting at a flow rate of 10 mL min<sup>-1</sup> with the following gradient: 0–5 min, isocratic A/B (100:0); 5–50 min, linear gradient from A/B (100:0) to A/B (50:50) (eluent A: H<sub>2</sub>O/MeCN/TFA, 95:5:0.1 v/v/v, eluent B: MeCN/H<sub>2</sub>O/TFA, 95:5:0.1 v/v/v).

### Synthesis

2-Alkylidenehydrazinecarboxylic acid benzyl esters **4a–g** were synthesized according to the procedure described by Bailey et al.<sup>[30]</sup> and used without further purification in the next step.

**2-Ethylidenehydrazinecarboxylic acid benzyl ester (4a):** Colorless solid (2.27 g, 98%); <sup>1</sup>H NMR (500 MHz, CDCl<sub>3</sub>):  $\delta = 1.77$  (d,  $J = 5.6$  Hz, 3H, CH<sub>3</sub>, *Z* isomer), 1.95 (d,  $J = 5.3$  Hz, 3H, CH<sub>3</sub>, *E* isomer), 5.20 (br s, 2H, OCH<sub>2</sub>), 6.80 (br s, 1H, N=CH, *Z* isomer), 7.17 (br s, 1H, N=CH, *E* isomer), 7.34 (m, 5H, aryl-H), 8.05 ppm (br s, 1H, NH), *E/Z* ratio: 70:30; MS (ESI):  $m/z$  (%): 214.9 [ $M + Na$ ]<sup>+</sup> (100).

**2-Propylidenehydrazinecarboxylic acid benzyl ester (4b):** Colorless solid (3.57 g, 72%); <sup>1</sup>H NMR (500 MHz, CDCl<sub>3</sub>):  $\delta = 1.06$  (t,  $J = 7.6$  Hz, 3H, CH<sub>3</sub>), 2.28 (m, 2H, CH<sub>2</sub>), 5.19 (br s, 2H, OCH<sub>2</sub>), 7.15 (br m, 1H, N=CH), 7.32 (m, 5H, aryl-H), 8.13 ppm (br s, 1H, NH), data given are for the *E* isomer (*E/Z* ratio: 81:19); MS (ESI):  $m/z$  (%): 229.0 [ $M + Na$ ]<sup>+</sup> (100).

**2-Butylidenehydrazinecarboxylic acid benzyl ester (4c):** Colorless solid (3.38 g, 98%); <sup>1</sup>H NMR (500 MHz, CDCl<sub>3</sub>):  $\delta = 0.93$  (t,  $J = 7.5$  Hz, 3H, CH<sub>3</sub>), 1.50 (m, 2H, CH<sub>2</sub>CH<sub>2</sub>), 2.25 (m, 2H, N=CHCH<sub>2</sub>), 5.20 (br s, 2H, OCH<sub>2</sub>), 7.12 (br s, 1H, N=CH), 7.33 (m, 5H, aryl-H), 7.93 ppm (br s, 1H, NH), data given are for the *E* isomer (*E/Z* ratio: 79:21); MS (ESI):  $m/z$  (%): 243.0 [ $M + Na$ ]<sup>+</sup> (39).

**2-Pentylidenehydrazinecarboxylic acid benzyl ester (4d):** Pale yellow solid (3.68 g, 83%); <sup>1</sup>H NMR (500 MHz, CDCl<sub>3</sub>):  $\delta = 0.82$  (t,  $J = 7.3$  Hz, 3H, CH<sub>3</sub>), 1.25 (m, 2H, CH<sub>2</sub>), 1.43 (m, 2H, CH<sub>2</sub>), 2.24 (m, 2H, N=CHCH<sub>2</sub>), 5.17 (br s, 2H, OCH<sub>2</sub>), 7.14 (br m, 1H, N=CH), 7.31 (m, 5H, aryl-H), 8.30 ppm (br s, 1H, NH), data given are for the *E* isomer (*E/Z* ratio: 81:19); MS (ESI):  $m/z$  (%): 257.1 [ $M + Na$ ]<sup>+</sup> (100).

**2-Hexylidenehydrazinecarboxylic acid benzyl ester (4e):** Colorless solid (7.20 g, 99%); <sup>1</sup>H NMR (500 MHz, CDCl<sub>3</sub>):  $\delta = 0.84$  (t,  $J = 6.7$  Hz, 3H, CH<sub>3</sub>), 1.29 (m, 4H, 2 × CH<sub>2</sub>), 1.47 (m, 2H, CH<sub>2</sub>), 2.27 (m, 2H, N=CHCH<sub>2</sub>), 5.20 (br s, 2H, OCH<sub>2</sub>), 7.14 (br m, 1H, N=CH), 7.33 (m, 5H, aryl-H), 7.99 ppm (br s, 1H, NH), data given are for the *E* isomer (*E/Z* ratio: 79:21); MS (ESI):  $m/z$  (%): 271.1 [ $M + Na$ ]<sup>+</sup> (100).

**2-(Propan-2-ylidene)hydrazinecarboxylic acid benzyl ester (4f):** Colorless solid (3.21 g, 99%); <sup>1</sup>H NMR (500 MHz, CDCl<sub>3</sub>):  $\delta = 1.78$  (s, 3H, CH<sub>3</sub>), 2.03 (s, 3H, CH<sub>3</sub>), 5.22 (s, 2H, OCH<sub>2</sub>), 7.35 (m, 5H, aryl-H), 7.62 ppm (br s, 1H, NH); MS (ESI):  $m/z$  (%): 207.0 [ $M + H$ ]<sup>+</sup> (73).

**2-(2-Methylpropylidene)hydrazinecarboxylic acid benzyl ester (4g):** Colorless solid (3.42 g, 99%); <sup>1</sup>H NMR (500 MHz, CDCl<sub>3</sub>):  $\delta = 1.07$  (d,  $J = 6.8$  Hz, 6H, 2 × CH<sub>3</sub>), 2.57 (m, 1H, CH), 5.20 (br s, 2H, OCH<sub>2</sub>), 7.01 (br m, 1H, N=CH), 7.33 (m, 5H, aryl-H), 7.93 ppm (br s, 1H, NH), exclusively the *E* isomer is visible; MS (ESI):  $m/z$  (%): 243.0 [ $M + Na$ ]<sup>+</sup> (66).

1-Alkylhydrazine-1,2-dicarboxylic acid 2-benzyl 1-*tert*-butyl esters **6a–g** were synthesized according to the procedure described by Bailey et al.<sup>[30]</sup> In the case of ketimine **4f**, NaBH<sub>4</sub> was used instead of DIBAL for the reduction.

**1-Ethylhydrazine-1,2-dicarboxylic acid 2-benzyl 1-*tert*-butyl ester (6a):** Colorless oil (1.15 g, 37% over two steps);  $R_f = 0.8$  (*n*-hexane/EtOAc 2:1, v/v); <sup>1</sup>H NMR (500 MHz, CDCl<sub>3</sub>):  $\delta = 1.13$  (br t,  $J = 6.8$  Hz, 3H, CH<sub>3</sub>), 1.41 (br s, 9H, C(CH<sub>3</sub>)<sub>3</sub>), 3.51 (br s, 2H, NCH<sub>2</sub>), 5.16 (s, 2H, OCH<sub>2</sub>), 6.36 (br s, 1H, NH, *Z* isomer), 6.59 (br s, 1H, NH, *E* isomer), 7.34 ppm (m, 5H, aryl-H); MS (ESI):  $m/z$  (%): 317.1 [ $M + Na$ ]<sup>+</sup> (100).

**1-Propylhydrazine-1,2-dicarboxylic acid 2-benzyl 1-*tert*-butyl ester (6b):** Colorless oil (1.31 g, 29% over two steps);  $R_f = 0.8$  (*n*-hexane/EtOAc 3:1, v/v); <sup>1</sup>H NMR (500 MHz, CDCl<sub>3</sub>):  $\delta = 0.88$  (m, 3H, CH<sub>3</sub>), 1.40 (br s, 9H, C(CH<sub>3</sub>)<sub>3</sub>), 1.56 (m, 2H, CH<sub>2</sub>CH<sub>3</sub>), 3.42 (m, 2H, NCH<sub>2</sub>), 5.15 (s, 2H, OCH<sub>2</sub>), 6.31 (br s, 1H, NH, *Z* isomer), 6.54 (br s, 1H, NH, *E* isomer), 7.34 ppm (m, 5H, aryl-H); MS (ESI):  $m/z$  (%): 331.2 [ $M + Na$ ]<sup>+</sup> (100).

**1-Butylhydrazine-1,2-dicarboxylic acid 2-benzyl 1-*tert*-butyl ester (6c):** Colorless oil (935 mg, 23% over two steps);  $R_f = 0.6$  (*n*-hexane/EtOAc 3:1, v/v); <sup>1</sup>H NMR (500 MHz, CDCl<sub>3</sub>):  $\delta = 0.90$  (m, 3H, CH<sub>3</sub>), 1.26–1.56 (m, 13H, C(CH<sub>3</sub>)<sub>3</sub>, CH<sub>2</sub>CH<sub>2</sub>), 3.45 (m, 2H, NCH<sub>2</sub>), 5.15 (s, 2H, OCH<sub>2</sub>), 6.32 (br s, 1H, NH, *Z* isomer), 6.54 (br s, 1H, NH, *E* isomer), 7.34 ppm (m, 5H, aryl-H); MS (ESI):  $m/z$  (%): 345.2 [ $M + Na$ ]<sup>+</sup> (83).

**1-Pentylhydrazine-1,2-dicarboxylic acid 2-benzyl 1-*tert*-butyl ester (6d):** Colorless oil (578 mg, 24% over two steps);  $R_f = 0.6$  (*n*-hexane/EtOAc 3:1, v/v); <sup>1</sup>H NMR (500 MHz, CDCl<sub>3</sub>):  $\delta = 0.83$  (t,  $J = 6.7$  Hz, 3H, CH<sub>3</sub>), 1.21–1.54 (m, 15H, C(CH<sub>3</sub>)<sub>3</sub>, CH<sub>2</sub>CH<sub>2</sub>CH<sub>2</sub>), 3.40 (s, 2H, NCH<sub>2</sub>), 5.11 (s, 2H, OCH<sub>2</sub>), 6.32 (br s, 1H, NH, *Z* isomer), 6.53 (s, 1H, NH, *E* isomer), 7.30 ppm (m, 5H, aryl-H); MS (ESI):  $m/z$  (%): 359.2 [ $M + Na$ ]<sup>+</sup> (68).

**1-Hexylhydrazine-1,2-dicarboxylic acid 2-benzyl 1-*tert*-butyl ester (6e):** Colorless oil (960 mg, 87% over two steps);  $R_f = 0.5$  (*n*-hexane/EtOAc 3:1, v/v); <sup>1</sup>H NMR (500 MHz, CDCl<sub>3</sub>):  $\delta = 0.84$  (m, 3H, CH<sub>3</sub>), 1.18–1.52 (m, 17H, C(CH<sub>3</sub>)<sub>3</sub>, CH<sub>2</sub>CH<sub>2</sub>CH<sub>2</sub>CH<sub>2</sub>), 3.42 (s, 2H, NCH<sub>2</sub>), 5.13 (s, 2H, OCH<sub>2</sub>), 6.52–6.92 (br m, 1H, NH, *E* and *Z* isomer), 7.32 ppm (m, 5H, aryl-H); MS (ESI):  $m/z$  (%): 373.2 [ $M + Na$ ]<sup>+</sup> (18).

**1-Isopropylhydrazine-1,2-dicarboxylic acid 2-benzyl 1-*tert*-butyl ester (6f):** Colorless oil (769 mg, 17% over two steps);  $R_f = 0.7$  (*n*-hexane/EtOAc 3:1, v/v); <sup>1</sup>H NMR (500 MHz, CDCl<sub>3</sub>):  $\delta = 1.10$  (br s, 6H, CH<sub>3</sub>), 1.40 (br s, 9H, C(CH<sub>3</sub>)<sub>3</sub>), 4.36 (br s, 1H, NCH), 5.15 (s, 2H, OCH<sub>2</sub>), 6.04 (br s, 1H, NH, *Z* isomer), 6.26 (br s, 1H, NH, *E* isomer), 7.35 ppm (m, 5H, aryl-H); MS (ESI):  $m/z$  (%): 331.2 [ $M + Na$ ]<sup>+</sup> (100).

**1-(2-Methylpropyl)hydrazine-1,2-dicarboxylic acid 2-benzyl 1-*tert*-butyl ester (6g):** Colorless oil (3.26 g, 66% over two steps);  $R_f = 0.7$  (*n*-hexane/EtOAc 3:1, v/v); <sup>1</sup>H NMR (500 MHz, CDCl<sub>3</sub>):  $\delta = 0.88$  (m, 6H, CH<sub>3</sub>), 1.32–1.53 (br m, 9H, C(CH<sub>3</sub>)<sub>3</sub>, *E* and *Z* isomer), 1.88 (m, 1H, CH), 3.27 (br s, 2H, NCH<sub>2</sub>), 5.15 (s, 2H, OCH<sub>2</sub>), 6.24–6.70 (br m, 1H, NH, *E* and *Z* isomer), 7.34 ppm (m, 5H, aryl-H); MS (ESI):  $m/z$  (%): 345.2 [ $M + Na$ ]<sup>+</sup> (100).

1-Alkylhydrazinecarboxylic acid *tert*-butyl esters **7a–g** were synthesized according to the procedure described by Bailey et al.<sup>[30]</sup> When

necessary, Boc-protected alkyldiazines were purified by flash chromatography after cleavage of the Z protecting group.

**1-Ethylhydrazinecarboxylic acid tert-butyl ester (7a):** Colorless oil (287 mg, 66%);  $R_f=0.4$  (*n*-hexane/EtOAc 3:1, *v/v*);  $^1\text{H NMR}$  (500 MHz,  $\text{CDCl}_3$ ):  $\delta=1.10$  (t,  $J=7.1$  Hz, 3H,  $\text{CH}_3$ ), 1.45 (s, 9H,  $\text{C}(\text{CH}_3)_3$ ), 3.38 (q,  $J=7.1$  Hz, 2H,  $\text{NCH}_2$ ), 3.69 ppm (br s, 2H,  $\text{NH}_2$ ); MS (ESI):  $m/z$  (%): 182.9 [ $M+\text{Na}$ ] $^+$  (61).

**1-Propylhydrazinecarboxylic acid tert-butyl ester (7b):** Colorless oil (204 mg, 79%);  $R_f=0.4$  (*n*-hexane/EtOAc 3:1, *v/v*);  $^1\text{H NMR}$  (500 MHz,  $\text{CDCl}_3$ ):  $\delta=0.85$  (t,  $J=7.4$  Hz, 3H,  $\text{CH}_3$ ), 1.45 (s, 9H,  $\text{C}(\text{CH}_3)_3$ ), 1.56 (m, 2H,  $\text{CH}_2\text{CH}_3$ ), 3.30 (t,  $J=7.1$  Hz, 2H,  $\text{NCH}_2$ ), 3.90 ppm (br s, 2H,  $\text{NH}_2$ ); MS (ESI):  $m/z$  (%): 197.0 [ $M+\text{Na}$ ] $^+$  (100). Data are in agreement with that reported by Park et al.<sup>[32]</sup>

**1-Butylhydrazinecarboxylic acid tert-butyl ester (7c):** Colorless oil (288 mg, 82%);  $R_f=0.3$  (*n*-hexane/EtOAc 3:1, *v/v*);  $^1\text{H NMR}$  (500 MHz,  $\text{CDCl}_3$ ):  $\delta=0.91$  (t,  $J=7.4$  Hz, 3H,  $\text{CH}_3$ ), 1.28 (m, 2H,  $\text{CH}_2\text{CH}_2\text{CH}_3$ ), 1.45 (s, 9H,  $\text{C}(\text{CH}_3)_3$ ), 1.52 (m, 2H,  $\text{CH}_2\text{CH}_2\text{CH}_3$ ), 3.34 (t,  $J=7.2$  Hz, 2H,  $\text{NCH}_2$ ), 3.94 ppm (br s, 2H,  $\text{NH}_2$ ); MS (ESI):  $m/z$  (%): 211.1 [ $M+\text{Na}$ ] $^+$  (79).

**1-Pentylhydrazinecarboxylic acid tert-butyl ester (7d):** Colorless oil (212 mg, 94%);  $R_f=0.3$  (petroleum ether/EtOAc 5:1, *v/v*);  $^1\text{H NMR}$  (500 MHz,  $\text{CDCl}_3$ ):  $\delta=0.87$  (t,  $J=7.2$  Hz, 3H,  $\text{CH}_3$ ), 1.22 (m, 2H,  $\text{CH}_2\text{CH}_2\text{CH}_2\text{CH}_3$ ), 1.30 (m, 2H,  $\text{CH}_2\text{CH}_2\text{CH}_2\text{CH}_3$ ), 1.44 (s, 9H,  $\text{C}(\text{CH}_3)_3$ ), 1.53 (m, 2H,  $\text{CH}_2\text{CH}_2\text{CH}_2\text{CH}_3$ ), 3.32 (t,  $J=7.2$  Hz, 2H,  $\text{NCH}_2$ ), 3.88 ppm (br s, 2H,  $\text{NH}_2$ ); MS (ESI):  $m/z$  (%): 225.0 [ $M+\text{Na}$ ] $^+$  (7).

**1-Hexylhydrazinecarboxylic acid tert-butyl ester (7e):** Colorless oil (142 mg, 29%);  $R_f=0.3$  (petroleum ether/EtOAc 5:1, *v/v*);  $^1\text{H NMR}$  (500 MHz,  $\text{CDCl}_3$ ):  $\delta=0.87$  (t,  $J=6.8$  Hz, 3H,  $\text{CH}_3$ ), 1.28 (m, 6H,  $\text{CH}_2\text{CH}_2\text{CH}_2\text{CH}_2\text{CH}_3$ ), 1.45 (s, 9H,  $\text{C}(\text{CH}_3)_3$ , *E* isomer), 1.48 (s, 9H,  $\text{C}(\text{CH}_3)_3$ , *Z* isomer), 1.64 (m, 2H,  $\text{CH}_2\text{CH}_2\text{CH}_2\text{CH}_2\text{CH}_3$ ), 3.50 ppm (t,  $J=7.5$  Hz, 2H,  $\text{NCH}_2$ ), signal for  $\text{NH}_2$  not visible; MS (ESI):  $m/z$  (%): 239.1 [ $M+\text{Na}$ ] $^+$  (58).

**1-Isopropylhydrazinecarboxylic acid tert-butyl ester (7f):** Colorless oil (179 mg, 63%);  $R_f=0.6$  (*n*-hexane/EtOAc 4:1, *v/v*);  $^1\text{H NMR}$  (500 MHz,  $\text{CDCl}_3$ ):  $\delta=1.09$  (d,  $J=6.6$  Hz, 6H,  $\text{CH}_3$ ), 1.45 (s, 9H,  $\text{C}(\text{CH}_3)_3$ ), 3.49 (br s, 2H,  $\text{NH}_2$ ), 4.19 ppm (br m, 1H, CH); MS (ESI):  $m/z$  (%): 197.0 [ $M+\text{Na}$ ] $^+$  (55).

**1-(2-Methylpropyl)hydrazinecarboxylic acid tert-butyl ester (7g):** Colorless oil (124 mg, 21%);  $R_f=0.3$  (*n*-hexane/EtOAc 5:1, *v/v*);  $^1\text{H NMR}$  (500 MHz,  $\text{CDCl}_3$ ):  $\delta=0.85$  (d,  $J=6.7$  Hz, 6H,  $\text{C}(\text{CH}_3)_2$ ), 1.44 (s, 9H,  $\text{C}(\text{CH}_3)_3$ ), 1.97 (m, 1H, CH), 3.15 (d,  $J=7.3$  Hz, 2H,  $\text{NCH}_2$ ), 3.94 ppm (br s, 2H,  $\text{NH}_2$ ); MS (ESI):  $m/z$  (%): 211.0 [ $M+\text{Na}$ ] $^+$  (100).

**General procedure for the synthesis of inhibitors 1, 8–15:** A solution of E-64c (75 mg, 0.24 mmol), TBTU (77 mg, 0.24 mmol), and DIPEA (41  $\mu\text{L}$ , 0.24 mmol) in  $\text{CH}_2\text{Cl}_2$  (5 mL) was treated with hydrazinecarboxylic acid tert-butyl ester (0.36 mmol, 1.5 equiv) dissolved in  $\text{CH}_2\text{Cl}_2$  (2 mL). In the case of inhibitor 1, EDC and HOBt were used instead of TBTU for the coupling step. The solution was stirred at RT for 3 h. Then, the solvent was removed in vacuo, and the obtained residue distributed between EtOAc (30 mL) and  $\text{H}_2\text{O}$  (10 mL). The resulting organic phase was washed with 5% aq  $\text{KHSO}_4$  (3  $\times$  10 mL), 5% aq  $\text{NaHCO}_3$  (5  $\times$  10 mL), and brine (1  $\times$  10 mL), and then dried ( $\text{Na}_2\text{SO}_4$ ), and concentrated in vacuo. The protected inhibitor was isolated as a colorless powder by precipitation from EtOAc/*n*-hexane and subjected to deprotection without further purification. For this, the protected inhibitor was dissolved at RT in TFA/ $\text{H}_2\text{O}$  (95:5, *v/v*; 2 mL). After 30 min, the inhibitor was isolated as the TFA salt by adding the cleavage solution dropwise to ice-cold tert-butyl methyl ether/petroleum ether (1:2, *v/v*;

100 mL). The obtained precipitate was collected by centrifugation, washed with petroleum ether (3  $\times$  10 mL), and dried in vacuo. If necessary, the inhibitor was further purified by RP-HPLC.

**(2S,3S)-3-(Hydrazinecarbonyl)-N-((S)-1-(isopentylamino)-4-methyl-1-oxopentan-2-yl)oxirane-2-carboxamide (1):** Colorless solid (21 mg, 22% over two steps); HPLC:  $t_R=6.9$  min;  $^1\text{H NMR}$  (500 MHz,  $[\text{D}_6]\text{DMSO}$ ):  $\delta=0.80\text{--}0.91$  (m, 12H,  $\delta\text{-CH}_3$  Leu,  $\delta\text{-CH}_3$  *i*-amyl), 1.27 (m,  $J=5$  Hz, 2H,  $\beta\text{-CH}_2$  *i*-amyl), 1.45 (m, 2H,  $\beta\text{-CH}_2$  Leu), 1.54 (m, 2H,  $\gamma\text{-CH}$  Leu,  $\gamma\text{-CH}$  *i*-amyl), 3.01 (m, 1H,  $\alpha\text{-CH}_2$  *i*-amyl), 3.07 (m, 1H,  $\alpha\text{-CH}_2$  *i*-amyl), 3.60 (m, 1H, CH oxirane), 3.71 (m, 1H, CH oxirane), 4.30 (m, 1H,  $\alpha\text{-CH}$  Leu), 8.04 (t,  $J=5.6$  Hz, 1H, NH *i*-amyl), 8.63 ppm (d,  $J=8.2$  Hz, 1H, NH Leu), signals for  $\text{NHNH}_2$  are not visible; HRMS (MALDI):  $m/z$  [ $2M+\text{Na}$ ] $^+$  calcd for  $(\text{C}_{15}\text{H}_{28}\text{N}_4\text{O}_4)_2\text{Na}$ : 679.41133, found: 679.41196.

**(2S,3S)-N-((S)-1-(isopentylamino)-4-methyl-1-oxopentan-2-yl)-3-(2-methylhydrazinecarbonyl)oxirane-2-carboxamide (8):** Colorless solid (79 mg, 60% over two steps); HPLC:  $t_R=6.9$  min;  $^1\text{H NMR}$  (500 MHz,  $[\text{D}_6]\text{DMSO}$ ):  $\delta=0.82\text{--}0.91$  (m, 12H,  $\delta\text{-CH}_3$  Leu,  $\delta\text{-CH}_3$  *i*-amyl), 1.26 (m, 2H,  $\beta\text{-CH}_2$  *i*-amyl), 1.44 (m, 2H,  $\beta\text{-CH}_2$  Leu), 1.54 (m, 2H,  $\gamma\text{-CH}$  Leu,  $\gamma\text{-CH}$  *i*-amyl), 2.62 (s, 3H,  $\text{NHCH}_3$ ), 3.01 (m, 1H,  $\alpha\text{-CH}_2$  *i*-amyl), 3.07 (m, 1H,  $\alpha\text{-CH}_2$  *i*-amyl), 3.54 (d,  $J=1.5$  Hz, 1H, CH oxirane), 3.71 (d,  $J=1.6$  Hz, 1H, CH oxirane), 4.30 (m, 1H,  $\alpha\text{-CH}$  Leu), 8.05 (t,  $J=5.5$  Hz, 1H, NH *i*-amyl), 8.62 (d,  $J=8.4$  Hz, 1H, NH Leu), 10.86 ppm (br s, 1H,  $\text{NHNHCH}_3$ ), signal for  $\text{NHNHCH}_3$  is not visible; HRMS (MALDI):  $m/z$  [ $M+\text{Na}$ ] $^+$  calcd for  $\text{C}_{16}\text{H}_{30}\text{N}_4\text{O}_4\text{Na}$ : 365.21593, found: 365.21631.

**(2S,3S)-3-(2-Ethylhydrazinecarbonyl)-N-((S)-1-(isopentylamino)-4-methyl-1-oxopentan-2-yl)oxirane-2-carboxamide (9):** Colorless solid (95 mg, 83% over two steps); HPLC:  $t_R=6.9$  min;  $^1\text{H NMR}$  (500 MHz,  $[\text{D}_6]\text{DMSO}$ ):  $\delta=0.82\text{--}0.91$  (m, 12H,  $\delta\text{-CH}_3$  Leu,  $\delta\text{-CH}_3$  *i*-amyl), 1.11 (t,  $J=7.2$  Hz,  $\beta\text{-CH}_3$  Et), 1.27 (m, 2H,  $\beta\text{-CH}_2$  *i*-amyl), 1.44 (m, 2H,  $\beta\text{-CH}_2$  Leu), 1.52 (m, 2H,  $\gamma\text{-CH}$  Leu,  $\gamma\text{-CH}$  *i*-amyl), 2.96–3.13 (m, 4H,  $\alpha\text{-CH}_2$  *i*-amyl,  $\alpha\text{-CH}_2$  Et), 3.63 (d,  $J=1.5$  Hz, 1H, CH oxirane), 3.74 (d,  $J=1.5$  Hz, 1H, CH oxirane), 4.31 (m, 1H,  $\alpha\text{-CH}$  Leu), 8.07 (t,  $J=5.5$  Hz, 1H, NH *i*-amyl), 8.68 (d,  $J=8.4$  Hz, 1H, NH Leu), 11.30 ppm (br s, 1H,  $\text{NHNHCH}_2$ ), signal for  $\text{NHNHCH}_2$  is not visible; HRMS (MALDI):  $m/z$  [ $M+\text{Na}$ ] $^+$  calcd for  $\text{C}_{17}\text{H}_{32}\text{N}_4\text{O}_4\text{Na}$ : 379.23158, found: 379.23138.

**(2S,3S)-N-((S)-1-(isopentylamino)-4-methyl-1-oxopentan-2-yl)-3-(2-propylhydrazinecarbonyl)oxirane-2-carboxamide (10):** Colorless solid (86 mg, 80% over two steps); HPLC:  $t_R=7.5$  min;  $^1\text{H NMR}$  (500 MHz,  $[\text{D}_6]\text{DMSO}$ ):  $\delta=0.81\text{--}0.92$  (m, 15H,  $\delta\text{-CH}_3$  Leu,  $\delta\text{-CH}_3$  *i*-amyl,  $\gamma\text{-CH}_3$  *n*-Pr), 1.27 (m, 2H,  $\beta\text{-CH}_2$  *i*-amyl), 1.44 (m, 2H,  $\beta\text{-CH}_2$  Leu), 1.53 (m, 4H,  $\gamma\text{-CH}$  Leu,  $\gamma\text{-CH}$  *i*-amyl,  $\beta\text{-CH}_2$  *n*-Pr), 2.91 (m, 2H,  $\alpha\text{-CH}_2$  *n*-Pr), 3.01 (m, 1H,  $\alpha\text{-CH}_2$  *i*-amyl), 3.07 (m, 1H,  $\alpha\text{-CH}_2$  *i*-amyl), 3.60 (d,  $J=1.5$  Hz, 1H, CH oxirane), 3.73 (d,  $J=1.5$  Hz, 1H, CH oxirane), 4.31 (m, 1H,  $\alpha\text{-CH}$  Leu), 8.06 (t,  $J=5.5$  Hz, 1H, NH *i*-amyl), 8.65 (d,  $J=8.5$  Hz, 1H, NH Leu), 11.11 ppm (br s, 1H,  $\text{NHNHCH}_2$ ), signal for  $\text{NHNHCH}_2$  is not visible; HRMS (MALDI):  $m/z$  [ $M+\text{H}$ ] $^+$  calcd for  $\text{C}_{18}\text{H}_{35}\text{N}_4\text{O}_4$ : 371.26528, found: 371.26567.

**(2S,3S)-3-(2-Butylhydrazinecarbonyl)-N-((S)-1-(isopentylamino)-4-methyl-1-oxopentan-2-yl)oxirane-2-carboxamide (11):** Colorless solid (67 mg, 57% over two steps); HPLC:  $t_R=8.0$  min;  $^1\text{H NMR}$  (500 MHz,  $[\text{D}_6]\text{DMSO}$ ):  $\delta=0.81\text{--}0.92$  (m, 15H,  $\delta\text{-CH}_3$  Leu,  $\delta\text{-CH}_3$  *i*-amyl,  $\delta\text{-CH}_3$  *n*Bu), 1.27 (m, 2H,  $\beta\text{-CH}_2$  *i*-amyl), 1.31 (m, 2H,  $\gamma\text{-CH}_2$  *n*Bu), 1.45 (m, 4H,  $\beta\text{-CH}_2$  Leu,  $\beta\text{-CH}_2$  *n*Bu), 1.54 (m, 2H,  $\gamma\text{-CH}$  Leu,  $\gamma\text{-CH}$  *i*-amyl), 2.87 (m, 2H,  $\alpha\text{-CH}_2$  *n*Bu), 3.01 (m, 1H,  $\alpha\text{-CH}_2$  *i*-amyl), 3.07 (m, 1H,  $\alpha\text{-CH}_2$  *i*-amyl), 3.56 (d,  $J=1.8$  Hz, 1H, CH oxirane), 3.71 (d,  $J=1.8$  Hz, 1H, CH oxirane), 4.30 (m, 1H,  $\alpha\text{-CH}$  Leu), 8.05 (t,  $J=5.6$  Hz, 1H, NH *i*-amyl), 8.63 (d,  $J=8.4$  Hz, 1H, NH Leu), 10.79 ppm (br s, 1H,  $\text{NHNHCH}_2$ ), signal for  $\text{NHNHCH}_2$  is not visible; HRMS

(MALDI):  $m/z$   $[M+Na]^+$  calcd for  $C_{19}H_{36}N_4O_4Na$ : 407.26288, found: 407.26279.

**(2S,3S)-N-((S)-1-(Isopentylamino)-4-methyl-1-oxopentan-2-yl)-3-(2-pentylhydrazinecarbonyl)oxirane-2-carboxamide (12):** Colorless lyophilisate (19 mg, 19% over two steps); HPLC:  $t_R$  = 8.5 min;  $^1H$  NMR (500 MHz,  $[D_6]DMSO$ ):  $\delta$  = 0.81–0.90 (m, 15H,  $\delta$ -CH<sub>3</sub> Leu,  $\delta$ -CH<sub>3</sub> *i*-amyl,  $\epsilon$ -CH<sub>3</sub> *n*-Pn), 1.21–1.31 (m, 6H,  $\beta$ -CH<sub>2</sub> *i*-amyl,  $\gamma$ -CH<sub>2</sub> *n*-Pn,  $\delta$ -CH<sub>2</sub> *n*-Pn), 1.36–1.48 (m, 4H,  $\beta$ -CH<sub>2</sub> Leu,  $\beta$ -CH<sub>2</sub> *n*-Pn), 1.54 (m, 2H,  $\gamma$ -CH Leu,  $\gamma$ -CH *i*-amyl), 2.72 (t,  $J$  = 7.1 Hz, 2H,  $\alpha$ -CH<sub>2</sub> *n*-Pn), 2.96–3.12 (m, 2H,  $\alpha$ -CH<sub>2</sub> *i*-amyl), 3.48 (d,  $J$  = 1.8 Hz, 1H, CH oxirane), 3.67 (d,  $J$  = 1.8 Hz, 1H, CH oxirane), 4.29 (m, 1H,  $\alpha$ -CH Leu), 8.03 (t,  $J$  = 5.6 Hz, 1H, NH *i*-amyl), 8.59 (d,  $J$  = 8.4 Hz, 1H, NH Leu), 10.13 ppm (s, 1H, NHNHCH<sub>2</sub>), signal for NHNHCH<sub>2</sub> is not visible; HRMS (ESI):  $m/z$   $[M+H]^+$  calcd for  $C_{20}H_{39}N_4O_4$ : 399.29710, found: 399.2966.

**(2S,3S)-3-(2-Hexylhydrazinecarbonyl)-N-((S)-1-(isopentylamino)-4-methyl-1-oxopentan-2-yl)oxirane-2-carboxamide (13):** Colorless lyophilisate (36 mg, 38% over two steps); HPLC:  $t_R$  = 9.2 min;  $^1H$  NMR (500 MHz,  $[D_6]DMSO$ ):  $\delta$  = 0.81–0.91 (m, 15H,  $\delta$ -CH<sub>3</sub> Leu,  $\delta$ -CH<sub>3</sub> *i*-amyl,  $\xi$ -CH<sub>3</sub> *n*-Hex), 1.20–1.32 (m, 8H,  $\beta$ -CH<sub>2</sub> *i*-amyl,  $\gamma$ -CH<sub>2</sub> *n*-Hex,  $\delta$ -CH<sub>2</sub> *n*-Hex,  $\epsilon$ -CH<sub>2</sub> *n*-Hex), 1.37–1.49 (m, 4H,  $\beta$ -CH<sub>2</sub> Leu,  $\beta$ -CH<sub>2</sub> *n*-Hex), 1.54 (m, 2H,  $\gamma$ -CH Leu,  $\gamma$ -CH *i*-amyl), 2.74 (m, 2H,  $\alpha$ -CH<sub>2</sub> *n*-Hex), 2.97–3.12 (m, 2H,  $\alpha$ -CH<sub>2</sub> *i*-amyl), 3.49 (d,  $J$  = 1.5 Hz, 1H, CH oxirane), 3.67 (d,  $J$  = 1.6 Hz, 1H, CH oxirane), 4.30 (m, 1H,  $\alpha$ -CH Leu), 8.02 (t,  $J$  = 5.5 Hz, 1H, NH *i*-amyl), 8.58 (d,  $J$  = 8.4 Hz, 1H, NH Leu), 10.21 ppm (s, 1H, NHNHCH<sub>2</sub>), signal for NHNHCH<sub>2</sub> is not visible; HRMS (ESI):  $m/z$   $[M+H]^+$  calcd for  $C_{21}H_{41}N_4O_4$ : 413.31275, found: 413.3124.

**(2S,3S)-N-((S)-1-(Isopentylamino)-4-methyl-1-oxopentan-2-yl)-3-(2-isopropylhydrazinecarbonyl)oxirane-2-carboxamide (14):** Colorless solid (93 mg, 79% over two steps); HPLC:  $t_R$  = 7.2 min;  $^1H$  NMR (500 MHz,  $[D_6]DMSO$ ):  $\delta$  = 0.82–0.90 (m, 12H,  $\delta$ -CH<sub>3</sub> Leu,  $\delta$ -CH<sub>3</sub> *i*-amyl), 1.06 (d,  $J$  = 6.2 Hz, 6H, CH<sub>3</sub> *i*Pr), 1.27 (m, 2H,  $\beta$ -CH<sub>2</sub> *i*-amyl), 1.45 (m, 2H,  $\beta$ -CH<sub>2</sub> Leu), 1.55 (m, 2H,  $\gamma$ -CH Leu,  $\gamma$ -CH *i*-amyl), 3.01 (m, 1H,  $\alpha$ -CH<sub>2</sub> *i*-amyl), 3.07 (m, 1H,  $\alpha$ -CH<sub>2</sub> *i*-amyl), 3.20 (m, 1H, CH *i*Pr), 3.59 (d,  $J$  = 1.8 Hz, 1H, CH oxirane), 3.72 (d,  $J$  = 1.8 Hz, 1H, CH oxirane), 4.31 (m, 1H,  $\alpha$ -CH Leu), 8.06 (d,  $J$  = 5.5 Hz, 1H, NH *i*-amyl), 8.65 (d,  $J$  = 8.4 Hz, 1H, NH Leu), 10.71 ppm (br s, 1H, NHNHCH<sub>2</sub>), signal for NHNHCH<sub>2</sub> is not visible; HRMS (MALDI):  $m/z$   $[M+Na]^+$  calcd for  $C_{18}H_{34}N_4O_4Na$ : 393.24723, found: 393.24752.

**(2S,3S)-3-(2-Isobutylhydrazinecarbonyl)-N-((S)-1-(isopentylamino)-4-methyl-1-oxopentan-2-yl)oxirane-2-carboxamide (15):** Colorless solid (36 mg, 30% over two steps); HPLC:  $t_R$  = 8.0 min;  $^1H$  NMR (600 MHz,  $[D_6]DMSO$ ):  $\delta$  = 0.82–0.91 (m, 18H,  $\delta$ -CH<sub>3</sub> Leu,  $\delta$ -CH<sub>3</sub> *i*-amyl,  $\gamma$ -CH<sub>3</sub> *i*Bu), 1.27 (m, 2H,  $\beta$ -CH<sub>2</sub> *i*-amyl), 1.44 (m, 2H,  $\beta$ -CH<sub>2</sub> Leu), 1.54 (m, 2H,  $\gamma$ -CH Leu,  $\gamma$ -CH *i*-amyl), 1.72 (m, 1H,  $\beta$ -CH *i*Bu), 2.59 (m, 2H,  $\alpha$ -CH<sub>2</sub> *i*Bu), 3.01 (m, 1H,  $\alpha$ -CH<sub>2</sub> *i*-amyl), 3.07 (m, 1H,  $\alpha$ -CH<sub>2</sub> *i*-amyl), 3.49 (d,  $J$  = 1.8 Hz, 1H, CH oxirane), 3.67 (d,  $J$  = 1.8 Hz, 1H, CH oxirane), 4.29 (m, 1H,  $\alpha$ -CH Leu), 8.02 (d,  $J$  = 5.6 Hz, 1H, NH *i*-amyl), 8.57 (d,  $J$  = 8.4 Hz, 1H, NH Leu), 10.25 ppm (br s, 1H, NHNHCH<sub>2</sub>), signal for NHNHCH<sub>2</sub> is not visible; HRMS (MALDI):  $m/z$   $[M+Na]^+$  calcd for  $C_{19}H_{36}N_4O_4Na$ : 407.26288, found: 407.26269.

### Kinetic measurements

The enzymatic activity of cathepsin C (~50  $\mu$ M) and cathepsin L (~100  $\mu$ M) was measured using the fluorogenic substrate H-Ser-Tyr-7-amido-4-methylcoumarin (AMC) (50  $\mu$ M) and Z-Phe-Arg-AMC (5  $\mu$ M), respectively. The release of AMC was monitored continuously in a SFM 25 fluorimeter (Biotek Kontron, Neufahrn, Germany)

at excitation and emission wavelengths of 380 and 460 nm, respectively. After 5–10 min, that is, when a constant rate was established, test inhibitor was added, and the reaction was followed for up to 60 min. The pseudo-first-order rate constant ( $k_{obs}$ ) was obtained by fitting the observed pre-steady-state progress curve to the integrated equation of Morrison<sup>[33,34]</sup> with pro-Fit (Quantum-Soft, Uetikon am See, Switzerland) using a Levenberg–Marquardt algorithm. Apparent second-order rate constants were subsequently calculated as  $k_2/K_1 = k_{obs}/I_1$  from several independent experiments by linear regression and corrected for substrate competition.

### Model of E-64c-hydrazide (1) bound along the active-site cleft of cathepsin C

Using HyperChem (release 8.0.6), the X-ray crystal structures of cathepsin C in complex with the peptide-derived inhibitor H-Gly-Phe-CHN<sub>2</sub> (PDB code: 2DJF)<sup>[8]</sup> and the E-64-derived inhibitor NS-134 in complex with cathepsin B (PDB code: 1SP4)<sup>[35]</sup> were superimposed based on the conserved residues of the catalytic diad (Cys25 and His159; papain numbering). Upon removal of H-Gly-Phe-CHN<sub>2</sub>, E-64c-hydrazide (1) was positioned along the active-site cleft of cathepsin C utilizing NS-134 as a molecular scaffold. Finally, the geometry of the covalently bound E-64-hydrazide (1) was optimized using an AMBER force field (algorithm: steepest descent).

### Acknowledgements

Funding of N.S. by a Heisenberg Fellowship and of C.P.S. by project SO 249/1–1, priority program 1394 'Mast cells — promoters of health and modulator of diseases', of the Deutsche Forschungsgemeinschaft (DFG) is gratefully acknowledged.

**Keywords:** cathepsin C · dipeptidyl peptidase I (DPPI) · E-64 · hydrazines · papain-like cysteine proteases · structure–activity relationships

- [1] MEROPS, the Peptide Database, Sanger Institute, Wellcome Trust, UK; <http://merops.sanger.ac.uk/>.
- [2] B. Turk, D. Turk, I. Dolenc, V. Turk in *Handbook of Proteolytic Enzymes*, 2nd ed., vol. 2 (Eds.: A. J. Barrett, N. D. Rawlings, J. F. Woessner), Elsevier, London, 2004, pp. 1192–1196.
- [3] J. K. McDonald, P. X. Callahan, B. B. Zeitman, S. Ellis, *J. Biol. Chem.* **1969**, *244*, 6199–6208.
- [4] J. K. McDonald, B. B. Zeitman, S. Ellis, *Biochem. Biophys. Res. Commun.* **1972**, *46*, 62–70.
- [5] J. K. McDonald, B. B. Zeitman, T. J. Reilly, S. Ellis, *J. Biol. Chem.* **1969**, *244*, 2693–2709.
- [6] T. V. Tran, K. A. Ellis, C.-M. Kam, D. Hudig, J. C. Powers, *Arch. Biochem. Biophys.* **2002**, *403*, 160–170.
- [7] D. Turk, V. Janjic, I. Stern, M. Podobnik, D. Lamba, S. W. Dahl, C. Lauritzen, J. Pedersen, V. Turk, B. Turk, *EMBO J.* **2001**, *20*, 6570–6582.
- [8] A. Mølgaard, J. Arnau, C. Lauritzen, S. Larsen, G. Petersen, J. Pedersen, *Biochem. J.* **2007**, *401*, 645–650.
- [9] J. L. Schneck, J. P. Villa, P. McDevitt, M. S. McQueney, S. H. Thrall, T. D. Meek, *Biochemistry* **2008**, *47*, 8697–8710.
- [10] E. Kominami, K. Ishido, D. Muno, N. Sato, *Biol. Chem. Hoppe-Seyler* **1992**, *373*, 367–373.
- [11] C. T. N. Pham, R. J. Armstrong, D. B. Zimonjici, N. C. Popescui, D. G. Payan, T. J. Ley, *J. Biol. Chem.* **1997**, *272*, 10695–10703.
- [12] A. M. Adkison, S. Z. Raptis, D. G. Kelley, C. T. N. Pham, *J. Clin. Invest.* **2002**, *109*, 363–371.
- [13] C. T. N. Pham, T. J. Ley, *Proc. Natl. Acad. Sci. USA* **1999**, *96*, 8627–8632.

- [14] P. J. Wolters, C. T. N. Pham, D. J. Muilenburg, T. J. Ley, G. H. Caughey, *J. Biol. Chem.* **2001**, *276*, 18551–18556.
- [15] P. D. Sheth, J. Pedersen, A. F. Walls, A. R. McEuen, *Biochem. Pharmacol.* **2003**, *66*, 2251–2262.
- [16] Y. Hu, C. T. N. Pham, *Arthritis Rheum.* **2005**, *52*, 2553–2558.
- [17] M. B. Pagano, M. A. Bartoli, T. L. Ennis, D. Mao, P. M. Simmons, R. W. Thompson, C. T. N. Pham, *Proc. Natl. Acad. Sci. USA* **2007**, *104*, 2855–2860.
- [18] A. M. Akk, P. M. Simmons, H. W. Chan, E. Agapov, M. J. Holtzman, M. H. Grayson, C. T. N. Pham, *J. Immunol.* **2008**, *180*, 3535–3542.
- [19] T. C. Hart, P. S. Hart, M. D. Michalec, Y. Zhang, E. Firatli, T. E. Van Dyke, A. Stabholz, A. Zlorogorski, L. Shapira, W. A. Soskolne, *J. Med. Genet.* **2000**, *37*, 88–94.
- [20] C. T. Pham, J. L. Ivanovich, S. Z. Raptis, B. Zehnbauser, T. J. Ley, *J. Immunol.* **2004**, *173*, 7277–7281.
- [21] C.-M. Kam, M. G. Götz, G. Koot, M. McGuire, D. Thiele, D. Hudig, J. C. Powers, *Arch. Biochem. Biophys.* **2004**, *427*, 123–134.
- [22] D. Guay, C. Beaulieu, T. J. Reddy, R. Zamboni, N. Méthot, J. Rubin, D. Ethier, M. D. Percival, *Bioorg. Med. Chem. Lett.* **2009**, *19*, 5392–5396.
- [23] J. Bondebjerg, H. Fuglsang, K. R. Valeur, D. W. Kaznelson, J. Hansen, R. O. Pedersen, B. O. Krogh, B. S. Jensen, C. Lauritzen, G. Petersen, J. Pedersen, L. Nærum, *Bioorg. Med. Chem.* **2005**, *13*, 4408–4424.
- [24] J. C. Powers, J. L. Asgian, Ö. D. Ekici, K. E. James, *Chem. Rev.* **2002**, *102*, 4639–4750.
- [25] N. Schaschke, *J. Biotechnol.* **2007**, *129*, 308–315.
- [26] A. Yamamoto, K. Tomoo, K. Matsugi, T. Hara, Y. In, M. Murata, K. Kitamura, T. Ishida, *Biochim. Biophys. Acta Protein Struct. Mol. Enzymol.* **2002**, *1597*, 244–251.
- [27] A. J. Barrett, A. A. Kembhavi, M. A. Brown, H. Kirschke, C. G. Knight, M. Tamai, K. Hanada, *Biochem. J.* **1982**, *201*, 189–198.
- [28] N. Schaschke, I. Assfalg-Machleidt, W. Machleidt, D. Turk, L. Moroder, *Bioorg. Med. Chem.* **1997**, *5*, 1789–1797.
- [29] O. Busnel, L. Bi, H. Dali, A. Cheguillaume, S. Chevance, A. Bondon, S. Muller, M. Baudy-Floc'h, *J. Org. Chem.* **2005**, *70*, 10701–10708.
- [30] M. D. Bailey, T. Halmos, N. Goudreau, E. Lescop, M. Llinàs-Brunet, *J. Med. Chem.* **2004**, *47*, 3788–3799.
- [31] S. Takitani, Y. Asabe, T. Kato, M. Suzuki, Y. Ueno, *J. Chromatogr.* **1979**, *172*, 335–342.
- [32] S. O. Park, J. Kim, M. Koh, S. B. Park, *J. Comb. Chem.* **2009**, *11*, 315–326.
- [33] J. F. Morrison, *Trends Biochem. Sci.* **1982**, *7*, 102–105.
- [34] C. G. Knight in *Proteinase Inhibitors*, (Eds.: A. J. Barrett, G. Salvesen), Elsevier, Amsterdam, **1986**, pp. 23–51.
- [35] I. Stern, N. Schaschke, L. Moroder, D. Turk, *Biochem. J.* **2004**, *381*, 511–517.

---

Received: February 26, 2013

Published online on June 18, 2013